International Journal of Earth, Energy and Environmental Sciences
ISSN: 2517-942X
Vol:10, No:8, 2016

Application of Post-Stack and Pre-Stack Seismic Inversion for Prediction of Hydrocarbon Reservoirs in a Persian Gulf Gas Field

Nastaran Moosavi, Mohammad Mokhtari

Abstract**—**Seismic inversion is a technique which has been in use for years and its main goal is to estimate and to model physical characteristics of rocks and fluids. Generally, it is a combination of seismic and well-log data. Seismic inversion can be carried out through different methods; we have conducted and compared post-stack and pre- stack seismic inversion methods on real data in one of the fields in the Persian Gulf. Pre-stack seismic inversion can transform seismic data to rock physics such as P-impedance, S-impedance and density. While post- stack seismic inversion can just estimate P-impedance. Then these parameters can be used in reservoir identification. Based on the results of inverting seismic data, a gas reservoir was detected in one of Hydrocarbon oil fields in south of Iran (Persian Gulf). By comparing post stack and pre-stack seismic inversion it can be concluded that the pre-stack seismic inversion provides a more reliable and detailed information for identification and prediction of hydrocarbon reservoirs.

Keywords**—**Density, P-impedance, S-impedance, post-stack seismic inversion, pre-stack seismic inversion.

I. Introduction

SEISMIC inversion is a technique which transfers seismic data to rock physical properties to obtain an earth model. Post-stack and pre-stack inversion are two methods that we can analyze inversion results through. Reference [1] showed that if we assume that the recorded seismic signal is equal to the ratio of two layers impedance difference to their sum, then we can invert this equation to recover the P-impedance (the product of density and P-wave velocity). We can make predictions about lithology and porosity with P-impedance. Post-stack inversion theory can be extended to pre-stack inversion theory. Seismic traces as a function of angle can be given by the Aki-Richards equations [2]. Pre-stack inversion theory has been published in a less extensive form by Hampson et al. [3]. However, the theory builds on the work of Buland and Omre [4], who also use a small reflectivity approximation but do not use the same constraints, and also of Simmons and Backus [5], who use similar constraints but do not invert to impedance. More reliable information can be obtained through pre-stack inversion which we deal with S-impedance and density in addition to P-impedance. (and $\frac{Vp}{Vs}$ for a better evaluation). S-impedance (product of density and S-wave) is a good indicator for gas reservoirs. When P-wave enters a fluid volume, its amount drops dramatically, however S-wave remains unaffected.

Nastaran Moosavi is PhD student of Geophysics, Islamic Azad University, Science & Research Branch. Tehran, Iran (e-mail: nastaran.moosavi@gmail.com).

Mohammad Mokhtari is Professor of International Institute of Earthquake Engineering & Seismology, Tehran, Iran.

II. Geological Back Ground

The study area in NW of Persian Gulf is located at the northeastern edge of the Arabian Platform. Four structural trends (N-S, NE-SW, NW-SE and E-W) have been proposed for the Arabian Platform region based on the gravity studies conducted in early 1950's [6]. Aramco in 1959 proposed outlines of horsts (N-S and NE-SW trending structures, which is based on positive Bouger gravity anomaly beneath the Saudi Arabian oilfields and therefore, a series of basement-induced structures with a systematic spacing was suggested [7]. This pattern reflects the Precambrian basement architecture [8]. The basement fabrics also influenced not only the nature and thicknesses of the sedimentary cover but also affected the later constructional deformation during the Arabia-Eurasia collision.

The NE-SW trending Hendijan or Bahregansar High (also Nowruz-Hendijan Ridge) is a major structural element in the region where encompasses Arash and the neighboring Tangu, Hendijan, Bahregansar, Nowruz, Doura (Kuwaiti), Khafji and Safania (Saudi Arabian) fields, Fig. 1, the age of the Hendijan High is not clearly well-known, but this high was reactivated in Cretaceous time period considering its thickness variations across the high. In fact, the Hendijan high is the most striking lineament in NW Persian Gulf region. The appearance of this high seems to suggest a Hormuz Salt induced uplift over a reactivated basement lineament that formed during Cretaceous. In addition, a strike-slip fault zone is detectable parallel to the Hendijan High considering the seismic data.

A stratigraphic column of the area down to Lower Cretaceous contains mainly alteration of carbonate and clastic intervals (as reservoir layers) separated by evaporitic and argillaceous inter-beds. Uplifting, erosion and non-deposition caused considerable variations in thickness of some intervals (e.g., Sarvak Formation).

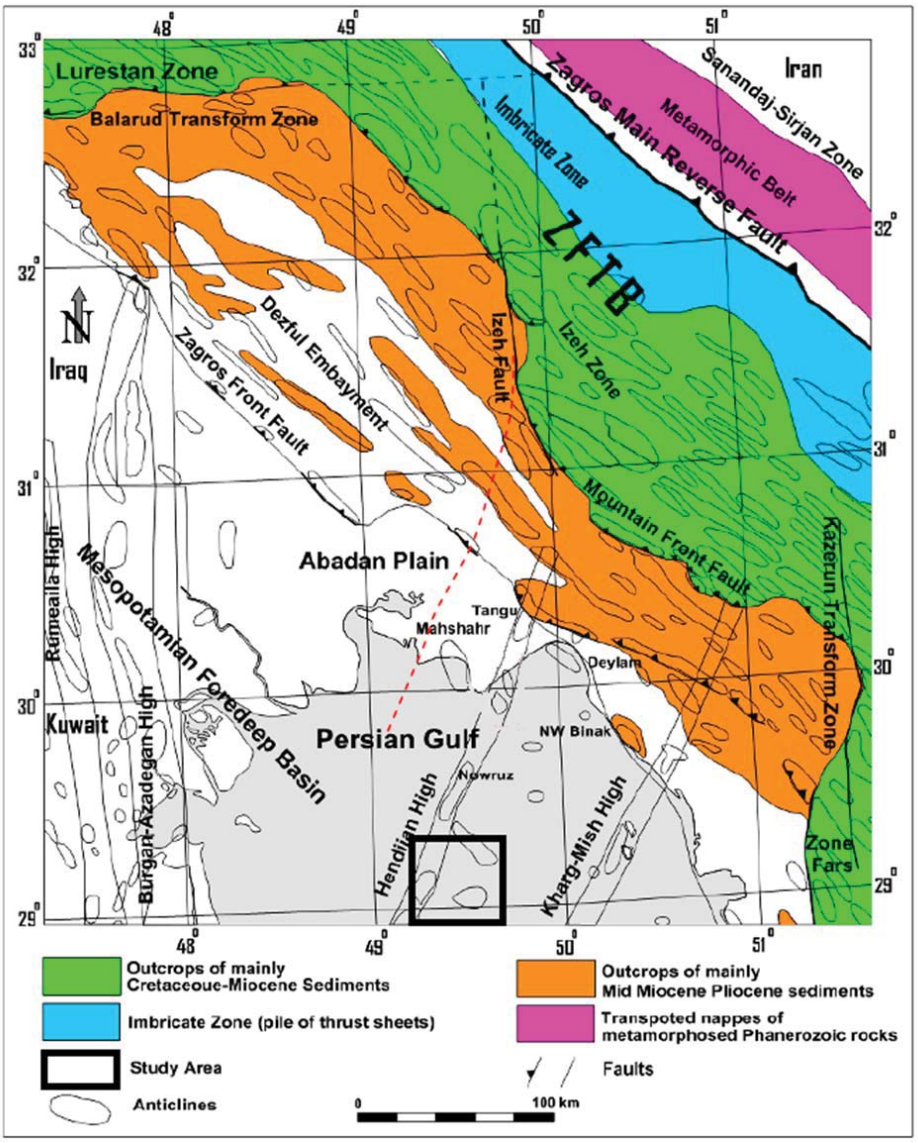

Fig. 1 Geological map of study area and major structural elements [9]

III. Post-Stack and Pre-Stack Seismic Data

We applied pre-stack and post-stack seismic data to study the reservoir in this area. When a seismic wave hits the interface of two volumes, it can convert to reflected and transmitted waves. This is called mode conversion, Fig. 2, and the amplitudes of the reflected and transmitted waves can be computed using the Zoeppritz equations [10].

In post-stack inversion we assume that seismic traces are zero offset. It means that they hit interface and reflect with zero angle. But in pre-stack seismic inversion we consider incident and reflected angles. Fig. 3 shows one NMO corrected common mid-point (CMP) gather before stacking (CMP gather NO3323 at well location). We see amplitude variations with offset. In Fig. 4, post-stack seismic traces are seen. Every trace is a CMP gather stack. Red ellipse in these two figures wants to show amplitude variations. In post-stack traces amplitude variations are almost steady. But in pre stack seismic data amplitude variations are more obvious.

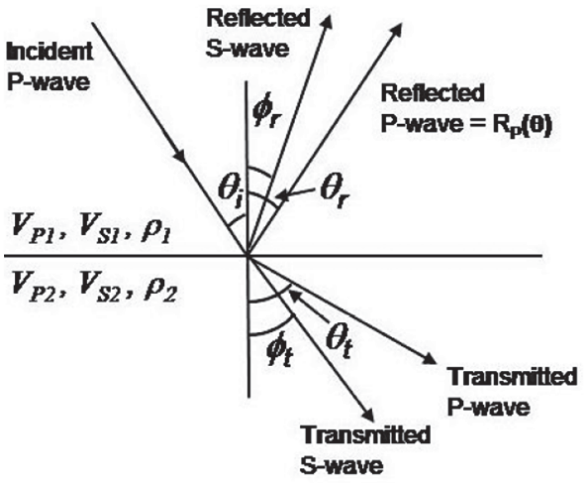

Fig. 2 When a wavefront hits a reflector with an incident angle, the part of the P-wave striking at the reflector will have its energy divided into reflected and transmitted P and S waves with the same angle, another part of the incident wave will have its energy broken up into P and S wave with a different angle of incidence which is called mode conversion [11]

Amplitude variations can be a good gas indicator. As we know reflection coefficient implies with equation $r=\frac{Ar}{Ai}$ (where A_r is amplitude of reflected wave and A_i is amplitude of incident wave). On the other hand, we imply reflection coefficient as equation:

$$r_{pi}=\frac{Zi+1-Zi}{Zi+1+Zi} \quad (1)$$

where r_{pi} is the zero offset reflection coefficient at the i^{th} interface and $Z_{pi}=\rho_i V_{pi}$ is the impedance of i^{th} layer. ρ is density and V_{pi} is P-wave velocity. When seismic wave enters a soft volume like gas regions, acoustic impedance decreases. So difference of acoustic impedance of two layers increases and reflection coefficient amount increases and leads to seismic amplitude increase. In this case, amplitude increase in seismic traces can be an indicator of gas presence. Pre-stack seismic data show amplitude variations much better than post-stack seismic data.

In this study, after a review of the geological background of the area, the pre- and post-stack seismic inversion has been briefly outlined and finally these techniques have been applied to real data.

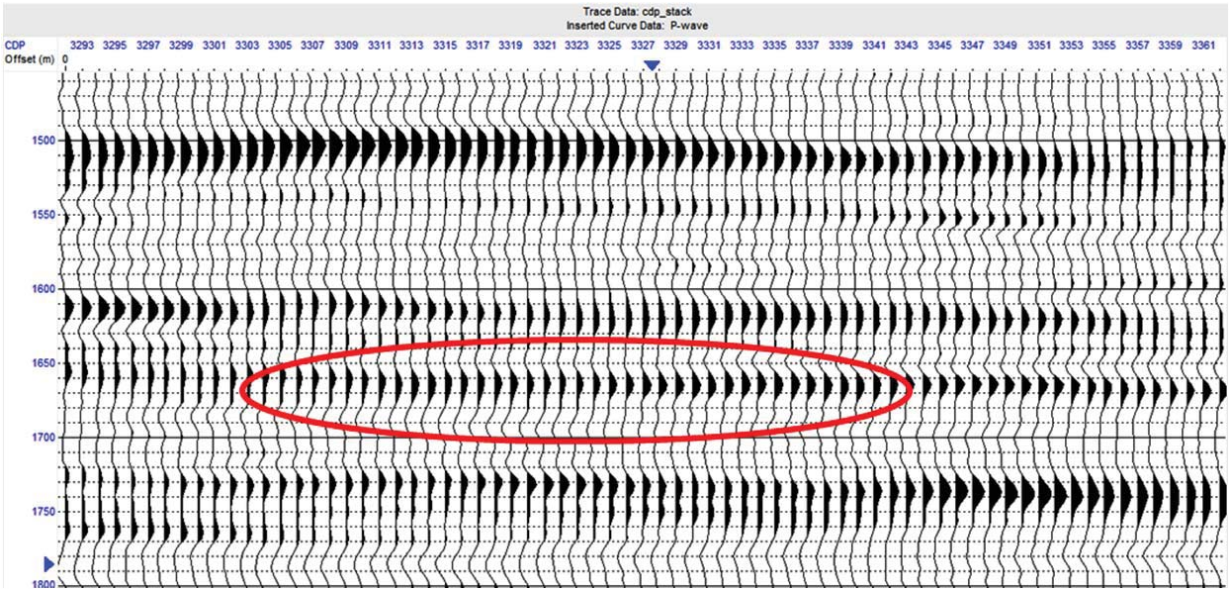

Fig. 3 Post-stack seismic section. Red ellipse shows amplitude variations of post-stack traces of study area. The amplitude variation in post-stack seismic data is not very sharp and is almost unchanged

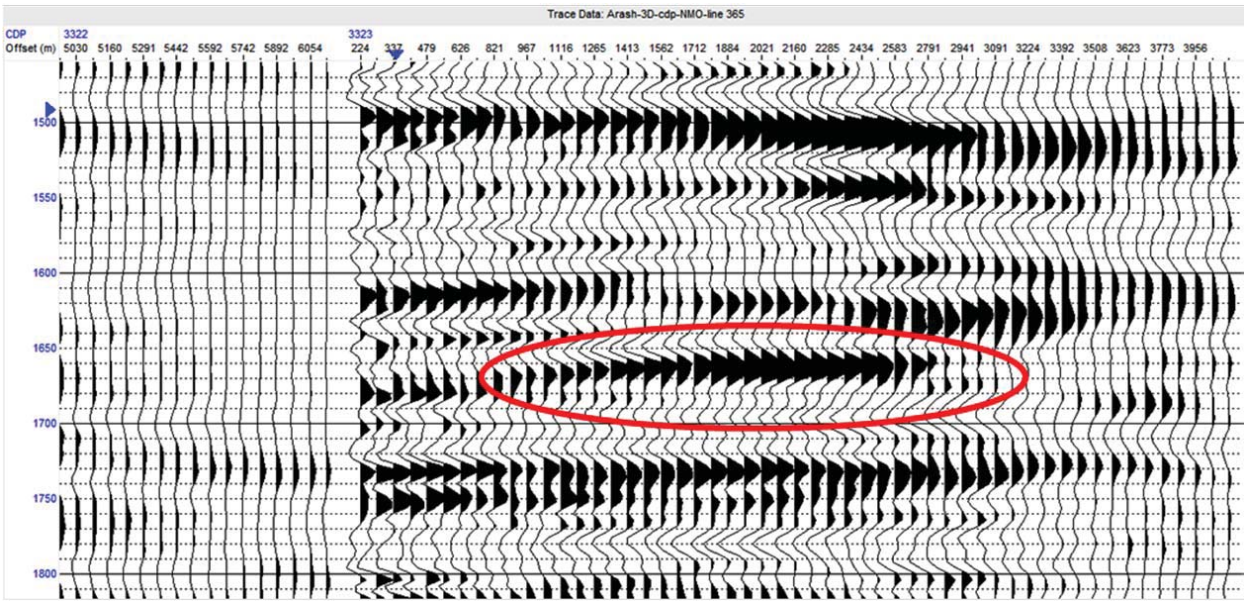

Fig. 4 Pre-stack seismic section. We can see part of NMO corrected CMP gather no3323. An amplitude variation with offset is obvious in the red ellipse

IV. Post-Stack Seismic Inversion

Post-stack seismic inversion is a technique which converts stacked seismic data to a P-impedance model. It is mainly based on one-dimensional convolutional model of s=w*r and reflectivity equation (1).

P-impedance can be extracted from (1), but the problem is that band limited wavelet removes low frequency component of reflectivity, so we need an initial P-impedance model from well log data to recover low frequencies [12]. Now we return to (1), assuming an amount of 0.1 or less for reflectivity, and using equation $Lpi=Ln(Zp_i)$, reflectivity can be written as $R=1/2DL_p$ or matrix form:

$$\begin{bmatrix} r_{P1} \\ r_{P2} \\ \vdots \\ r_{PN} \end{bmatrix} = \frac{1}{2} \begin{bmatrix} -1 & 1 & 0 & \cdots \\ 0 & -1 & 1 & \ddots \\ 0 & 0 & -1 & \ddots \\ \vdots & \ddots & \ddots & \ddots \end{bmatrix} \begin{bmatrix} L_{P1} \\ L_{P2} \\ \vdots \\ L_{PN} \end{bmatrix} \quad (2)$$

One-dimensional convolutional model s=w*r can also be written as matrix form:

$$\begin{bmatrix} s_1 \\ s_2 \\ \vdots \\ s_N \end{bmatrix} = \begin{bmatrix} W_1 & 0 & 0 & \cdots \\ W_2 & W_1 & 0 & \ddots \\ W_3 & W_2 & W_1 & \ddots \\ \vdots & \ddots & \ddots & \ddots \end{bmatrix} \begin{bmatrix} r_{P1} \\ r_{P2} \\ \vdots \\ r_{PN} \end{bmatrix} \quad (3)$$

With combining (2) and (3), an equation for inversion of post-stack seismic data can be concluded:

$$S=1/2WDL_p \quad (4)$$

where S is stacked seismic trace, W is wavelet matrix (3), D is derivative matrix in (2) and L_p is logarithm of P-impedance. At first we start with an initial model P-impedance, and then by using a standard matrix inversion, we estimate L_P with knowledge of the observed seismic trace and an extracted wavelet estimate. However, a full matrix inversion is both costly and potentially unstable, it is better to start with the initial guess impedance model and then iterate towards a solution using the conjugate gradient method [12].

V. Pre-Stack Inversion of Seismic Data

Now we can extend last section theory for pre-stack seismic inversion. In Post-stack inversion we assume that incident ray hits interface with a zero angle, but in pre-stack inversion incident angle is greater than zero, and a P-wave with incident angle θ, can convert to transmitted and reflected P and S waves. Zoeppritz equations determine amplitudes of these transmitted and reflected P and S waves. Aki-Richards equations [2] are linear conversions of Zoeppritz equations which were re-expressed by Fatti et al. [13]:

$$r_{pp}(\theta) = c_1 r_p + c_2 r_s + c_3 r_D \quad (5)$$

where $c_1 = 1+\tan^2\theta$ ، $c_2 = -8\gamma^2\tan^2\theta$ ، $c_3 = -0/5\tan^2\theta+2\gamma^2\sin^2\theta$ و $\gamma = \frac{vs}{vp}$ and $r_p = ½ [\frac{\Delta vp}{vp} + \frac{\Delta \rho}{\rho}]$ ، $r_s = ½ [\frac{\Delta vs}{vs} + \frac{\Delta \rho}{\rho}]$ و $r_D = \frac{\Delta \rho}{\rho}$.

Now we can extend (4) for S-impedance and density as $r_p = 1/2DL_p$ and $R_D = DL_D$. In pre-stack seismic inversion three parameters of P-impedance, S-impedance and density relate to each other with (6) and (7). To define unknown parameters in (6) and (7), we plot $Ln(Z_s)$ versus $Ln(Z_p)$ and $Ln(\rho)$ versus

$Ln(Z_p)$. k_c and m_c are determined from a best straight line fit of points in a logarithmic space, ΔL_D and ΔL_s are deviations away from this straight line, Fig. 5.

$$Ln(Z_s) = k * Ln(Z_p) + k_c + \Delta L_s \quad (6)$$

$$Ln(\rho) = m*Ln(Zp) + m_c + \Delta L_D \quad (7)$$

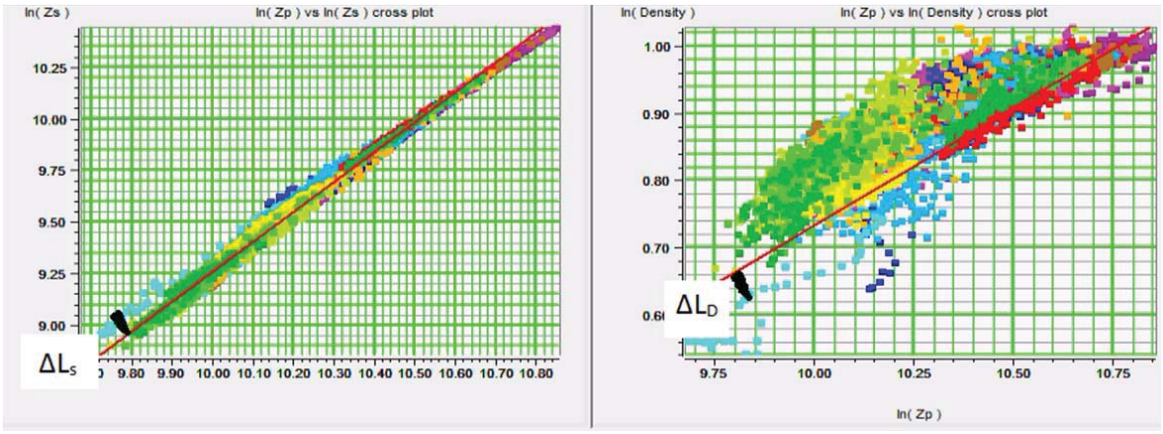

Fig. 5 Cross plots of Ln(ρ) versus Ln(Z_P) and Ln(Z_S) versus Ln(Z_P). In both cases there is a linear straight fit line and deviations away from the lines are ΔL_D and ΔL_s, but because they are small, we ignore their values

For a seismic trace dependent on angle $r_{pp}(\theta)$, we combine 1D convolutional model s=w*r with equation (4), to get a version of Fatti's equation then by using it with (6) and (7), we conclude simultaneous inversion equation:

$$S_\theta = \tilde{c}_1 W_\theta D L_p + \tilde{c}_2 W_\theta D \Delta L_s + W_\theta c_3 D \Delta L_D \quad (8)$$

where $\tilde{C}_1 = ½\ c_1 + 1/2kc_2 + mc_3$ and $\tilde{C}_2 = 1/2c_2$. Then we can estimate final amounts of P-impedance, S-impedance and density via equations $Z_p = \exp(L_p)$, $Z_s = \exp(kL_p + k_c + \Delta L_s)$ and $\rho = \exp(mL_p + m_c + \Delta L_D)$ [3].

VI. Real Data Example

The above mentioned techniques are being applied to a seismic profile extracted from a 3D seismic cub. The data has rather good quality and also a well is located in the vicinity of the used seismic line. Now in this part we need to extract suitable wavelets from seismic data. First we need to correlate seismic traces with well log data to recover frequencies we missed in seismic information. For post-stack seismic data, we extract one wavelet for the whole stacked seismic section after a good correlation of seismic and well data, Fig. 6. But in pre-stack seismic inversion in which Zoeppritz equations and their approximations are used, seismic traces are based on incident and reflected angles. So we should convert seismic traces from offset domain to angle domain. After division of seismic traces into different angles and correlation of well log and seismic data, we can extract one wavelet for each angle depending seismic trace group. Here we have sorted the data into three angle; 0^0-15^0, 15^0-30^0, 30^0- 45^0 and we extracted one wavelet for each groups, Fig. 6. The next step is to build initial models. We build initial models on seismic section at the location of well and then propagate it for the whole seismic profile.

Now it is time to invert the seismic data. Inversion parameters are obtained for pre-stack inversion. We ignore ΔL_D and ΔL_s, because they are small and near zero. k_c, k, m_c and m are calculated as k = 1.45103, k_c =-5.25181, m = 0.350746 and m_c = -2.77358. Fig. 7 is a comparison of initial models and inversion results. There is a good correlation between initial model and inversion results. Output for post-stack inversion is P-impedance Fig. 8 and for pre-stack inversion includes P-impedance, S-impedance and density, Fig. 9. Inversion is evaluated in area showed between two black lines. For study of lithology we use estimation of $\frac{Vp}{Vs}$ from pre-stack seismic inversion, Fig. 9.

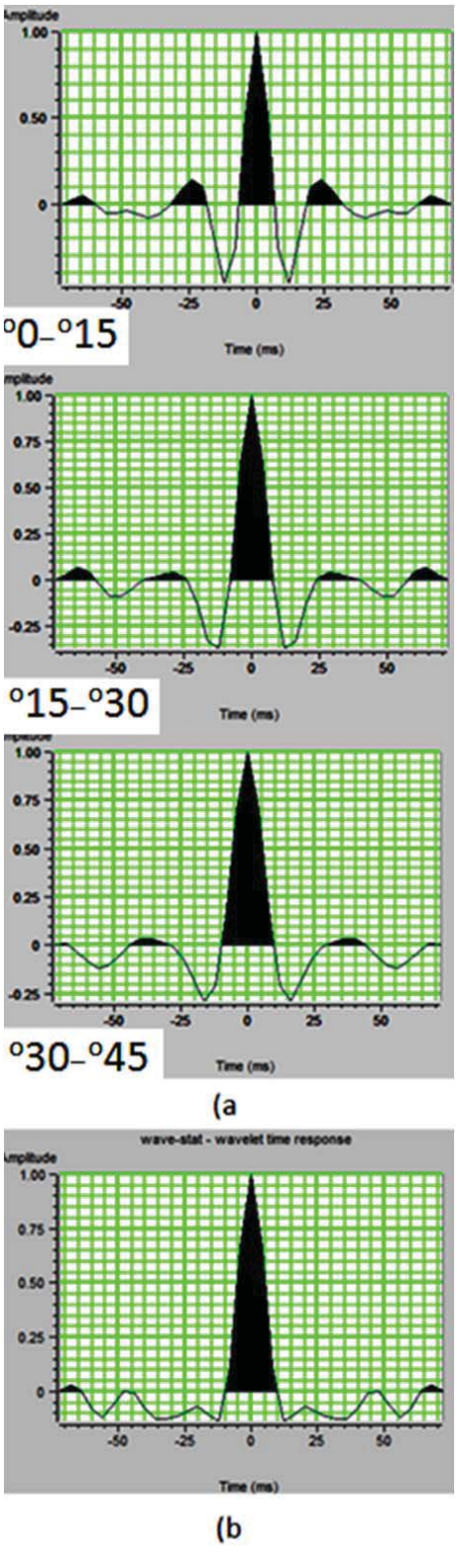

Fig. 6 (a) three wavelets extracted from angle dependent seismic group traces for pre-stack seismic inversion, (b) one wavelet extracted from the whole stacked seismic traces for post-stack seismic inversion

Results show that acoustic impedance obtained from both post-stack and pre-stack inversion is high in the study area. The study area is a carbonate formation and it is mainly made of limestone. Therefore, according to that, we expect that amounts of P-impedance, S-impedance and density to be high in this formation. We also estimated $\frac{Vp}{Vs}$ to get more information about lithology changes.

Fahliyan formation within the study area starts at around 1560 milliseconds in inverted seismic sections. For a better discussion we categorized inverted sections into three time range 1560-1630 ms, 1630-1700 ms and 1700-1740 ms.

Within the range of 1560-1630 ms, P-impedance from post-stack inversion and P-impedance, S-impedance and density from pre-stack inversion is high, which expected as it consisted of carbonate.

Within the range of 1630-1700 ms, we observe decrease in P-impedance from post-stack inversion and P-impedance, density and $\frac{Vp}{Vs}$ ratio from pre-stack inversion. However, the S-impedance distribution around this time range is almost constant and we see almost no obvious change in this area. As we know, shear velocity in fluids has no special change, but P-wave velocity drops as enters fluids, so we can conclude that shear velocity is a good indicator to identify gas presence. With comparing of what is said, we can predict a gas reservoir in case study region.

Within the range of 1700-1740 ms, we have increase in P-impedance from post-stack inversion and P-impedance, S-impedance and density from pre-stack inversion. $\frac{Vp}{Vs}$ ratio has a decrease at this time range. Again this can be because of carbonate type of Fahlyian formation [14].

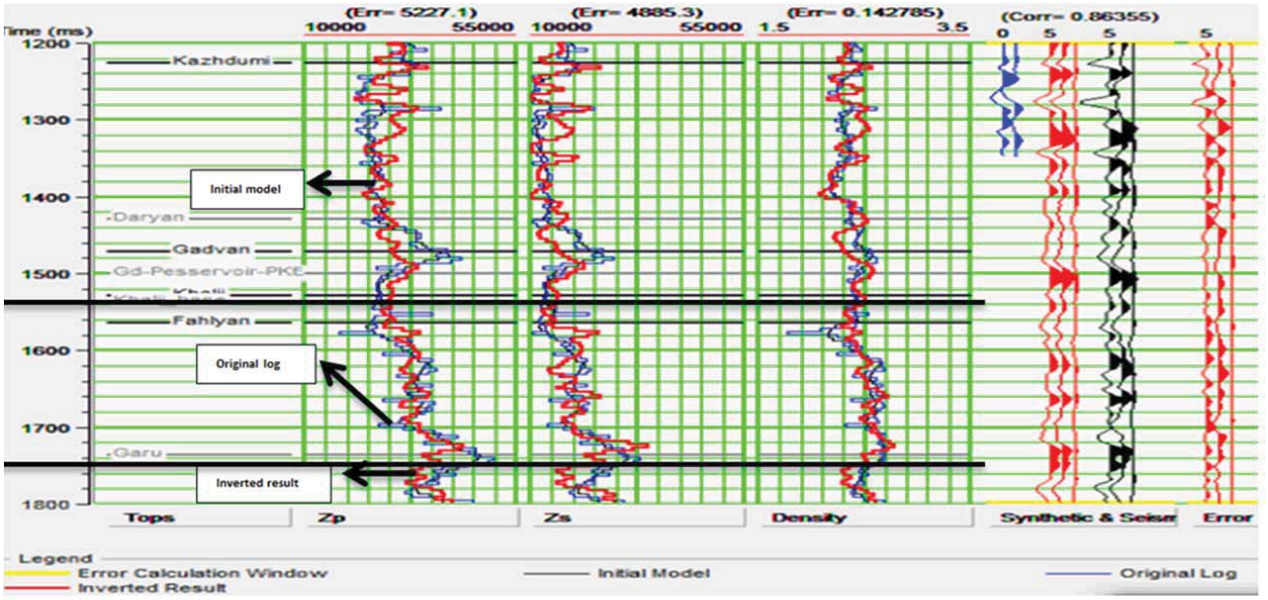

(a

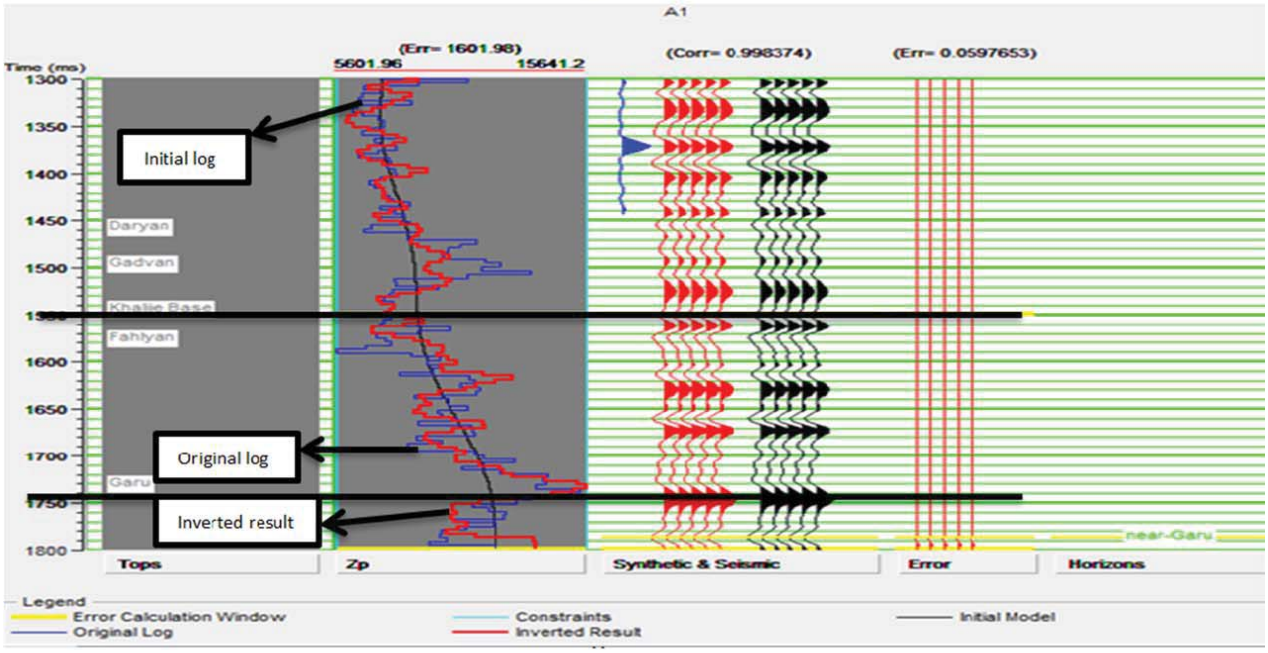

(b

Fig. 7 Inversion at well location, comparing inverted results with initial log. Red curve (inversion), blue curve (original log), black curve (initial log). Region of study is located between the two black lines. Pre-stack seismic inversion results are P-impedance, S-impedance and density a). Post-stack seismic inversion result is P-impedance b). There is a good correlation between blue and red curves

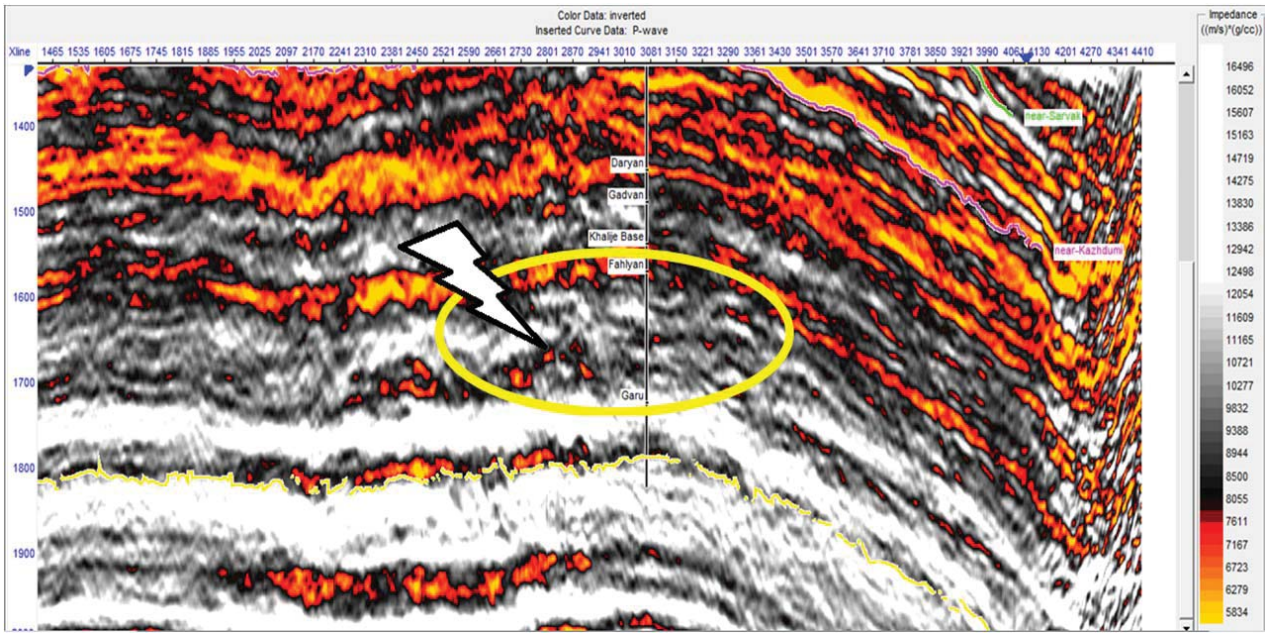

Fig. 8 P-impedance inversions from post-stack seismic data. The ellipse is the region of study. The arrow shows suggested gas location

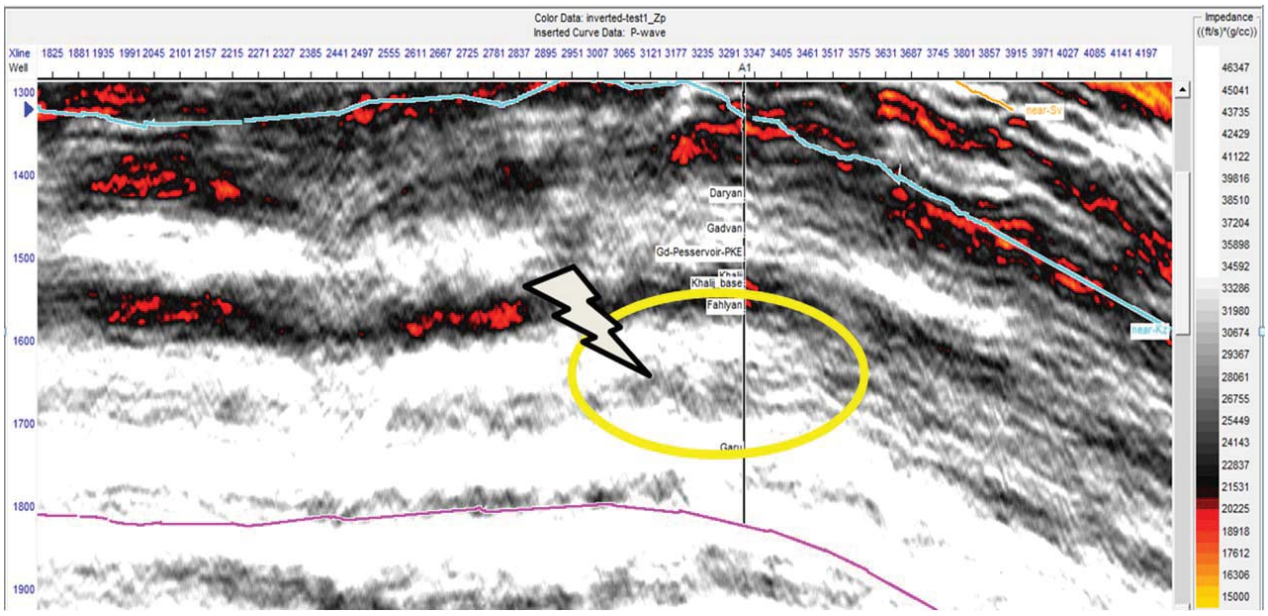

(a)

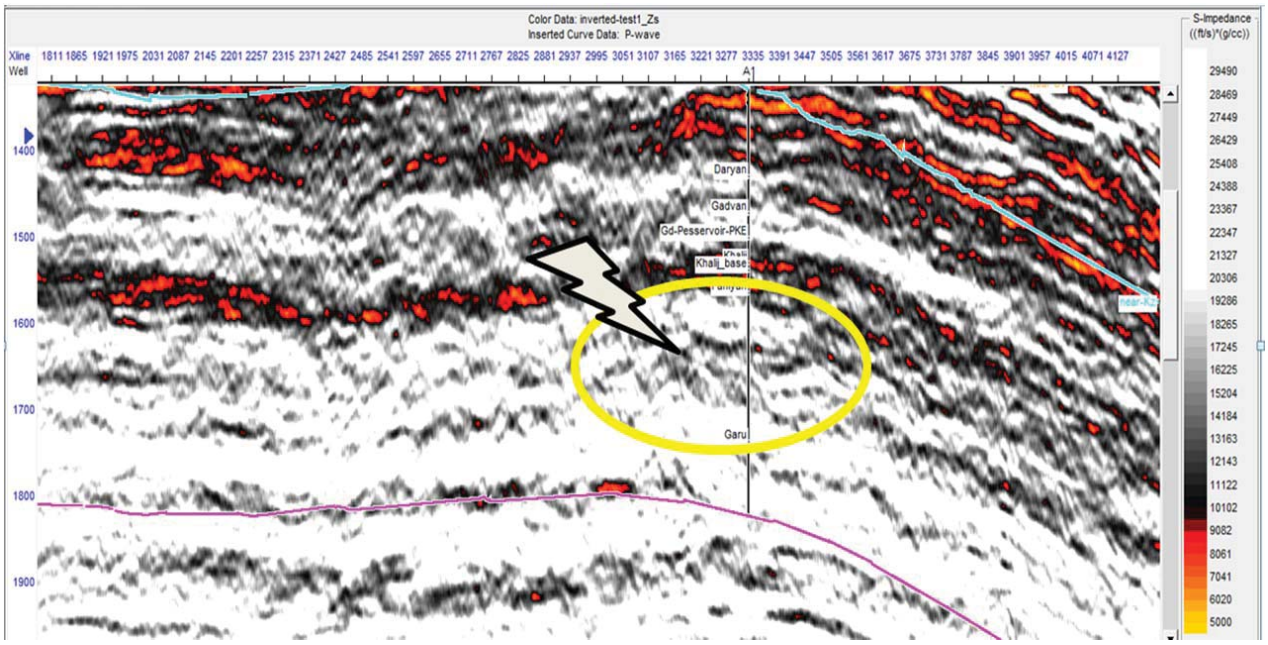
Color Data: inverted-test1_Zs
Inserted Curve Data: P-wave
S-Impedance ((ft/s)*(g/cc))
Xline
Well
A1
Daryan
Gadvan
Gd-Pesservoir-PKE
Khali_base
Garu
Near-Kaz

(b)

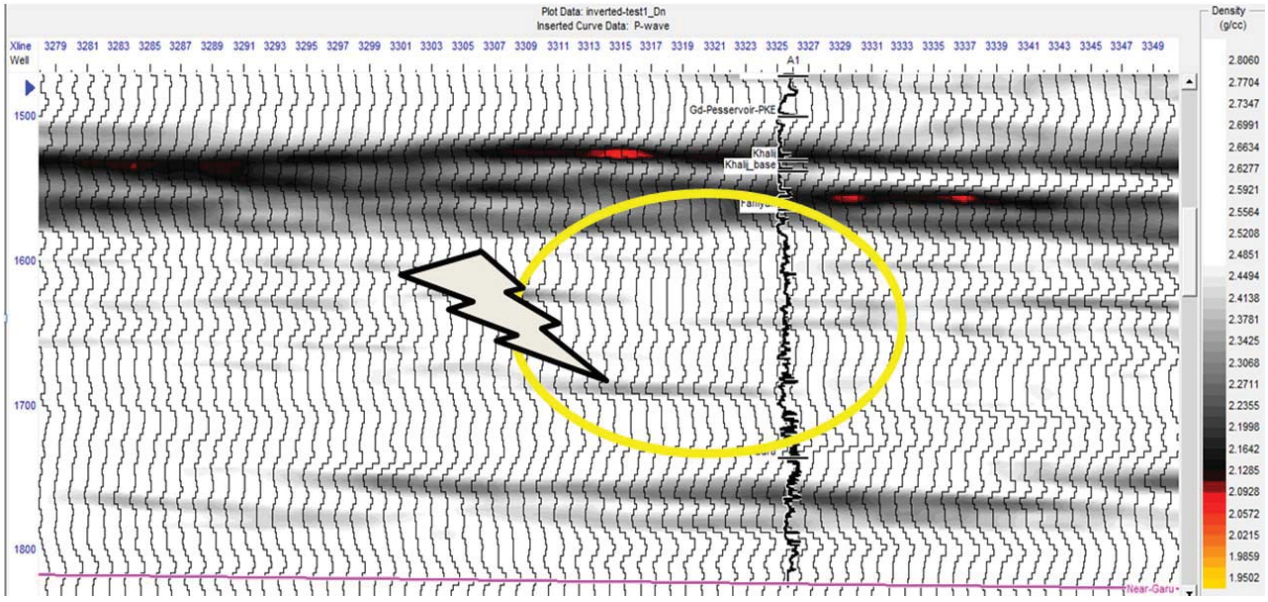
Plot Data: inverted-test1_Dn
Inserted Curve Data: P-wave
Density (g/cc)
Xline
Well
A1
Gd-Pesservoir-PKE
Khali_base
Near-Garu

(c)

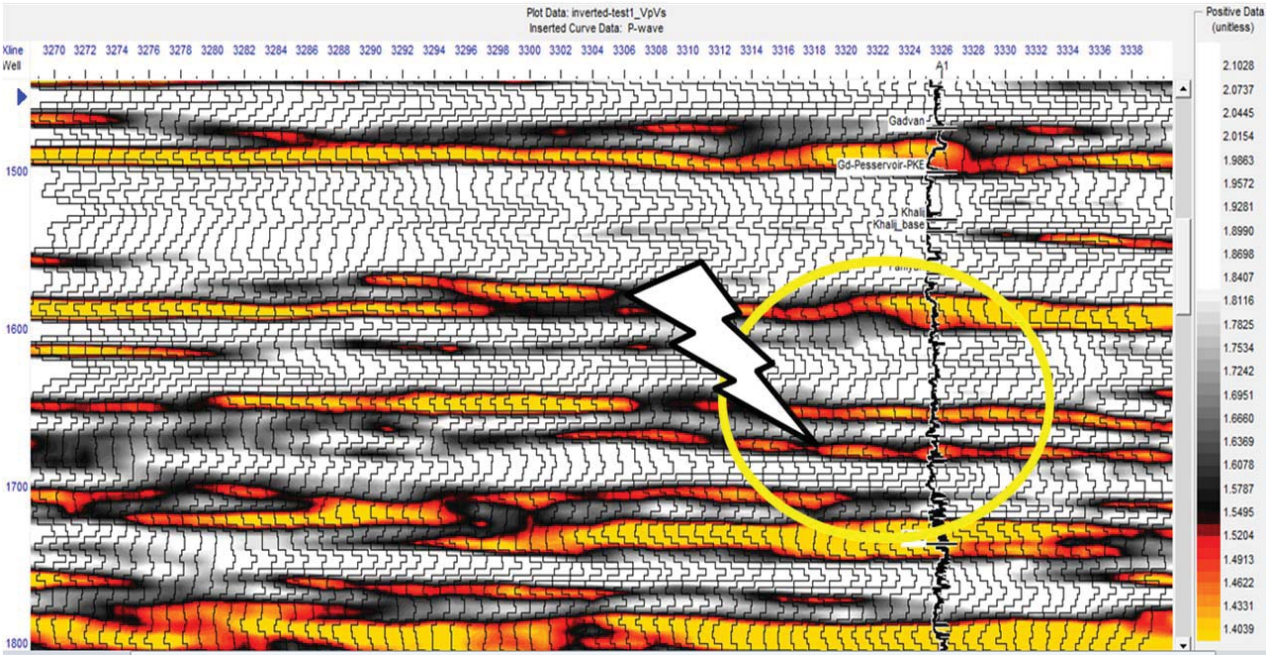

(d)

Fig. 9 (a) P-impedance; (b) S-impedance; (c) density and (d) $\frac{Vp}{Vs}$ ratio obtained from pre-stack seismic inversion. The ellipse is the region of study. The suggested gas location is being indicated by the arrow

VII. Conclusion

Here a comparison of post-stack and pre-stack inversion of seismic data in one of oil fields in the Persian Gulf has been conducted. Using the pre-stack seismic inversion technique we estimated three parameters of P-impedance, S-impedance and density. For a more exact evaluation we plotted $\frac{Vp}{Vs}$ ratio. Post-stack inversion resulted in P-impedance. We observed decrease in p-impedances and $\frac{Vp}{Vs}$ ratio, while S-impedance had little change. As shear wave velocity is not affected by fluids, so we know it is a good gas indicator. These reasons help us to suggest a gas reservoir in the study area. So we can see that pre-stack inversion provides us with more detailed and exact information as compared with post-stack and is a better method for study of gas reservoirs.

References

[1] Lindseth, R.O., 1979, Synthetic Sonic Logs – a process for stratigraphic interpretation, Geophysics, Vol. 44, p. 3-26.
[2] Aki, K., and Richards, P.G., 2002, Quantitative Seismology, 2nd Edition: W.H. Freeman and Company.
[3] Hampson, D., Russell, B., and Bankhead, B., 2005, Simultaneous inversion of prestack seismic data: Ann. Mtg. Society of Exploration Geophysics, Abstracts.
[4] Buland, A. and Omre, H., 2003, Bayesian linearized AVO inversion: Geophysics, Vol. 68, p. 185-198.
[5] Simmons, J.L. and Backus, M.M., 1996, Waveform-based AVO inversion and AVO prediction-error, Geophysics, Vol. 61, p. 1575-1588.
[6] Henson, F.R.S., 1951, Observations on the Geology and Petroleum Occurrences of the Middle East, 3rd World Petroleum Congress, The Hague, Proceedings, Section 1, p.118- 140.
[7] Edgell, H. S., 1996, Salt tectonism in the Persian Gulf Basin: in Alsop, I., Blundell, D., Davison, I., eds., Salt Tectonics, Special Publication no. 100. London: Geological
[8] Al-Husseini, M.I., 2000, Origin of the Arabian Plate Structures: Amar Collision and Najd Rift, GeoArabia, v. 5, p. 527-542.
[9] Abdollahie Fard, I., 2006, Structural models for the South Khuzestan area based on reflection seismic data, PhD Thesis, Shahid Beheshti University.
[10] Zoeppritz, K., 1919, Erdbebenwellen VIII B. Über Reflexion and durchgang seismischer wellen duch unstetigkeitsflachen, Gottinger Nachr. 1, p. 66-84.
[11] Sheriff, R.E, (1980), Seismic Stratigraphy. IHRDC Publishers.
[12] Russell, B.H., and Hampson, D.P., 1991, A comparison of post-stack seismic inversion methods: Ann. Mtg. Abstracts, SEG, p. 876-878.
[13] Fatti, J. L., Smith, G.C., Vail, P.J., Strauss, P.J., and Levitt, P.R., 1994, Detection of gas in sandstone reservoirs using AVO analysis: a 3D Seismic Case History Using the Geostack Technique: Geophysics, 59, 1362-1376.
[14] Moosavi, N.,2013, Application of pre-stack seismic inversion for study of hydrocarbon reservoir properties in one of the fields in south of Iran, MSC thesis, Islamic Azad University North Tehran Branch.